Optical and Quantum Electronics **34:** 145–159, 2002.

Design and optimization of 2D photonic crystal waveguides based on silicon

M.J.A. DE DOOD*, E. SNOEKS†, A. MOROZ‡ AND A. POLMAN
FOM Institute for Atomic and Molecular Physics, Kruislaan 407, 1098 SJ Amsterdam, The Netherlands
*(*author for correspondence, E-mail: m.d.dood@amolf.nl)*
(†Present address: Corus, Ijmuiden, The Netherlands)
(‡Present address: Debye Research Institute, Utrecht University, Padualaan 8, 3584 CH Utrecht, The Netherlands)

Abstract. The existence and properties of photonic band gaps was investigated for a square lattice of dielectric cylinders in air. Band structure calculations were performed using the transfer matrix method as function of the dielectric constant of the cylinders and the cylinder radius-to-pitch ratio r/a. It was found that band gaps exist only for transverse magnetic polarization for a dielectric contrast larger then 3.8 (index contrast >1.95). The optimum r/a ratio is 0.25 for the smallest index contrast. For silicon cylinders ($n = 3.45$) the widest gap is observed for $r/a = 0.18$. Band structure calculations as function of r/a show that up to four gaps open for the silicon structure. The effective index was obtained from the band structure calculations and compared with Maxwell–Garnett effective medium theory. Using the band structure calculations we obtained design parameters for silicon based photonic crystal waveguides. The possibility and limitations of amorphous silicon, silicon germanium and silicon-on-insulator structures to achieve index guiding in the third dimension is discussed.

Key words: photonic band gaps, photonic crystals, silicon, waveguide

1. Introduction

A photonic crystal is composed of a periodic arrangement of dielectric material in two or three dimensions. If the periodicity and symmetry of the crystal and the dielectric constants of the materials used are chosen well, the band structure of such a crystal shows a photonic band gap (PBG) for one or both polarizations, i.e. at particular frequencies light propagation is prohibited in any direction in the crystal. The possible applications of these photonic crystals are numerous, including inhibition and enhancement of spontaneous emission (Sprik *et al.* 1996; Megens *et al.* 1999), fabrication of sharp waveguide bends (Mekis *et al.* 1996; Lin *et al.* 1998), couplers and filters (Stoffer *et al.* 2000).

In three dimensions the fabrication of photonic crystals for optical frequencies relies mainly on self-assembly techniques. In two dimensions, lithography and anisotropic etching techniques can be used. Two-dimensional (2D) photonic crystals can be integrated with existing planar optical waveguide tech-

nology in which lithography and etching are used routinely for the fabrication of waveguides and other devices.

In two dimensions the only simple structure that offers a full PBG, i.e. a band gap overlapping for both transverse magnetic (TM) and transverse electric (TE) polarization, is a triangular array of holes (Winn *et al.* 1994). However, this structure is relatively difficult to fabricate with high aspect ratio because little open space is available in the lattice for the volatile etching products to escape. Therefore we will focus on structures made using cylinders. The need of a 90° waveguide led to the choice of a square lattice (Mekis *et al.* 1996; Lin *et al.* 1998; Baba *et al.* 1999; Tokushima *et al.* 2000). In a square lattice of cylinders band gaps only open up for TM polarization (E-field along the cylinder axis); for the TE polarization no band gaps are expected (Joannopoulos *et al.* 1995).

In this paper we describe calculations of the photonic and waveguiding properties of 2D photonic crystal slab waveguides based on a square lattice of dielectric cylinders in air. We want to explore the minimum requirements and tolerances for fabrication of devices based on silicon as a base material, operating around the standard telecommunication wavelength of 1.5 μm. In the considered structures, vertical confinement is provided by index guiding using either amorphous silicon (a-Si) or SiGe sections in the pillars, or by using silicon-on-insulator (SOI) materials. Waveguide properties are calculated based on dielectric waveguide theory in which the photonic crystal is incorporated using the effective dielectric constant derived from the calculated band structures.

2. Band structure calculations

Band structure calculations were performed for infinitely long cylinders placed on a square lattice, using the transfer matrix method (Pendry and MacKinnon 1992). The structure considered in our calculations is shown in Fig. 1. The cylinder radius r and pitch a are shown in the upper left corner of the figure. The right part shows the definition of TM and TE polarizations. The lower left corner shows the square unit cell in reciprocal space used for the band structure calculations. The Γ, X and M points of high symmetry in reciprocal space are shown. Due to the discretization method used in the calculation scheme, we have only calculated the band structure along the ΓX and XM directions. We will consider dielectric cylinders of dielectric constant ε embedded in a background with $\varepsilon = 1.0$.

Fig. 2 shows the result of a band structure calculation for a square lattice of silicon cylinders ($\varepsilon = 11.8$, refractive index $n = 3.45$) in air. The radius-to-pitch-ratio r/a was chosen to be 0.18 in this case. The vertical frequency scale is given in dimensionless units. These can be converted to ordinary units by specifying the pitch a and the vacuum wavelength λ of interest. Note that

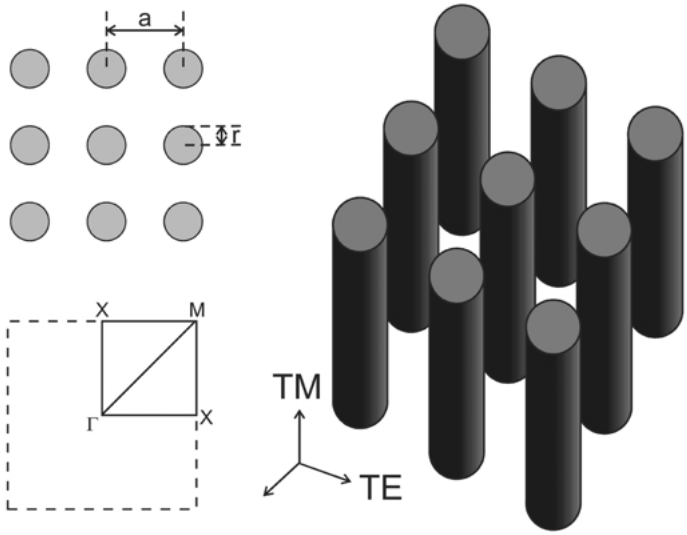

Fig. 1. Square lattice of dielectric cylinders. Indicated are the definition of the cylinder radius r and the pitch a. The Γ, X and M points of symmetry in the square Brillouin zone are indicated in the figure. The TE and TM polarizations are indicated in the right part of the figure, where the arrows indicate the direction of the electric field vector.

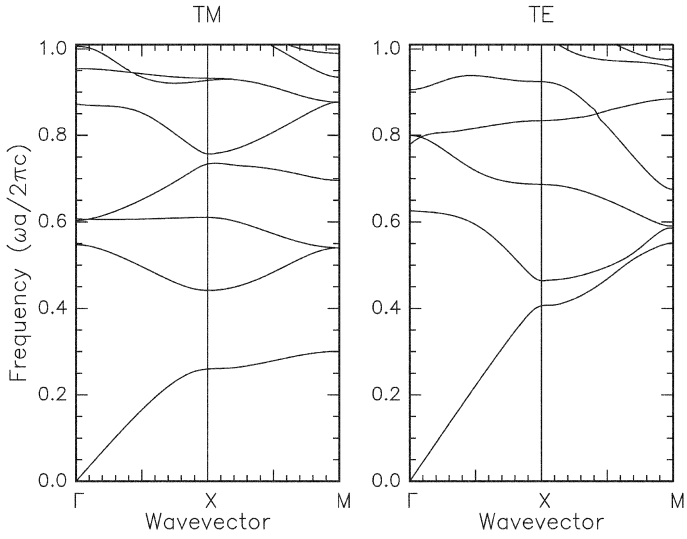

Fig. 2. Calculated band structure along the ΓX and XM directions for a square lattice of silicon cylinders ($\varepsilon = 11.8$) in air with $r/a = 0.18$, for TM and TE polarization. Due to the high index contrast a wide gap opens between the first and second band for TM polarization. For TE polarization no band gap is observed.

the use of dimensionless frequency is natural in the case of Maxwell's equations, because these equations do not define a fundamental length scale. Due to the high index contrast a wide gap opens between the first and second band for TM polarization. The gap extends from $\omega a/2\pi c = 0.30$ to 0.44, consistent with similar calculations for GaAs (Joannopoulos *et al.* 1995).

For TE polarization no band gaps are observed. This can be explained by considering the polarization of a cylinder induced by an external field. If the external electric field is directed along the long axis of the cylinder the cylinder is easily polarized resulting in a strong interaction of the cylinders with TM polarized waves, whereas for TE polarization the polarizability of the cylinder is small (Van de Hulst 1957).

Although we have calculated the band structure along the ΓX and XM directions only, the behavior along the ΓM direction can be predicted for the lower lying bands. Minima and maxima of a certain band are expected only at points of high symmetry in the reciprocal space. Therefore the part of the band along the missing ΓM direction varies smoothly between the minima and maxima already calculated at the Γ, X and M points. To design structures operating around 1.5 μm the pitch a should be chosen such that the desired wavelength falls in the band gap region. For a pitch of 570 nm, the midgap frequency corresponds to a wavelength of 1.536 μm.

Fig. 3 shows the dependence of the band gap frequencies on the pillar radius-to-pitch ratio r/a, extracted from band structure calculations as shown in Fig. 2. The solid dots indicate the maxima and minima observed in the bands of the calculated band structures for various values of r/a. The lines are smooth curves through the points to guide the eye. The area enclosed by the drawn lines indicates a band gap region. The first two band gaps could be mapped out in this way. Two higher bands for larger r/a are observed but not all points to map out the bands were calculated. The result of Fig. 3 can be compared to calculations for GaAs (Winn *et al.* 1994; Joannopoulos *et al.* 1995) and are found to be similar, because the refractive indices at 1.5 μm of GaAs and Si are similar.

The widest band gap for a lattice of silicon cylinders ($\varepsilon = 11.8$) is observed for $r/a = 0.20$, with a relative gap width of 38% (defined as the midgap frequency divided by the gap width). To find the minimum dielectric constant required for a band gap to occur in a square lattice for TM polarization, first a calculation as in Fig. 3 was repeated for cylinders with $\varepsilon = 4.0$. It was found that the widest gap in this case is observed for a r/a ratio of 0.25 (relative gap width 4%). Next, repeated band structure calculations as function of the dielectric constant of the cylinders at a fixed r/a of 0.25 were done. Fig. 4 shows the maximum frequency of the first band and the minimum frequency of the second band as function of ε. The region enclosed by the solid lines gives the gap between the first and second band. To find the minimum dielectric constant the solid lines were extrapolated, resulting in a

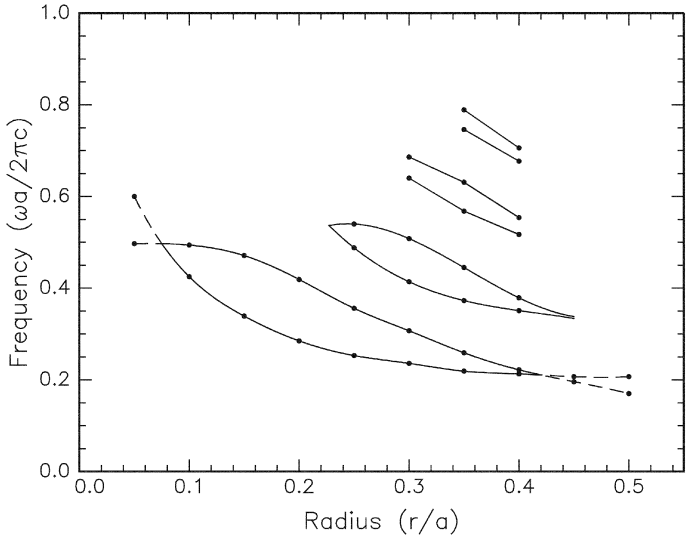

Fig. 3. Position of the band gaps for TM polarized light calculated for a square lattice of silicon cylinders in air. The positions of the gaps were extracted from band structure calculations at various values of r/a, depicted by the dots.

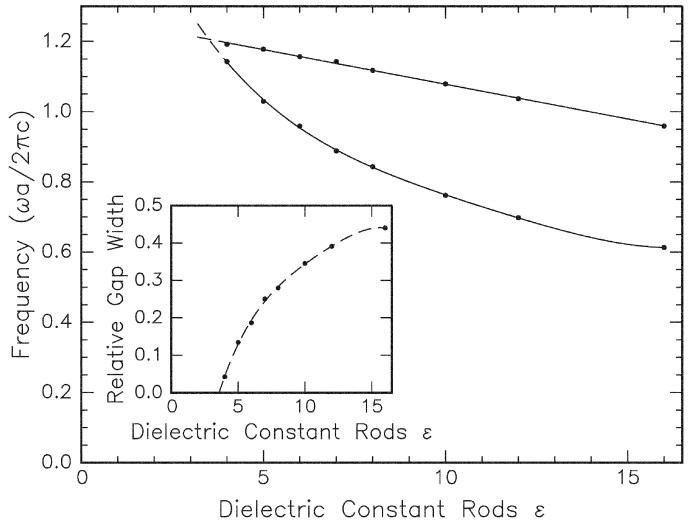

Fig. 4. Band gap between the first and second band for TM polarization for a square lattice of cylinders in air with $r/a = 0.25$ as function of the dielectric constant. A minimum dielectric constant of 3.8 ($n = 1.95$) is needed for gaps to open. The inset shows the same data plotted in terms of the relative gap width, defined as the gap width divided by the midgap frequency.

minimum dielectric constant of 3.8 ($n = 1.95$) for gaps to open for a square lattice of cylinders (dashed lines). The inset shows the same data plotted as

relative gap width. The upper frequency of the band gap, i.e. the minimum of the second band at the M point, decreased linearly with the ε of the cylinders.

The refractive index requirement of at least 1.95 for a gap to occur for the square lattice is just out of reach of standard polymers and glasses. The use of silicon as a base materials for 2D photonic crystals seems natural because of its high refractive index ($n = 3.45$) and because the microfabrication technology for this material is well characterized. For instance Si can be etched anisotropically to high precision using reactive ion etching (Tachi *et al.* 1991; Bartha *et al.* 1995; Zijlstra *et al.* 1999). The electronic band gap of silicon is 1.1 eV, corresponding to a wavelength of $\sim$1.1 μm in vacuum, yielding transparent silicon in the near-infrared.

3. 2D Photonic crystal waveguides

The structures discussed so far all consisted of cylinders of infinite length. For practical applications of 2D PBG materials, the photonic crystal must be incorporated into a waveguide structure. In a simple treatment the PBG effects take place in the plane of the photonic crystal, similar as in the case of infinitely long cylinders, while index guiding in the dielectric waveguide structure may be used to provide confinement of the light out of the plane of the photonic crystal. In this section we will describe the design of such structures using 2D band structure calculations combined with dielectric waveguide theory. Although this approach gives a good idea of the typical sizes and design parameters involved, only a full three-dimensional (3D) calculation can resolve the more detailed characteristics of such a device (Charlton *et al.* 1997; Charlton and Parker 1998; Astratov *et al.* 1999; Astratov *et al.* 1999; Johnson *et al.* 2000).

To treat a photonic crystal using ordinary waveguide theory, the effective index of a square lattice of silicon cylinders was evaluated as function of the fill fraction $f = \pi(r/a)^2$ of cylinders. The effective index is obtained in the long-wavelength limit from the linear part of the calculated dispersion relation near the zone center ($k = 0$):

$$n_{\text{eff}} = \lim_{k \to 0} c \left(\frac{\partial \omega}{\partial k} \right)^{-1}$$

As can be seen in Fig. 2 there is a large difference in effective index for TM and TE waves because of the difference in slope of the linear part of the dispersion relation near $k = 0$. Fig. 5 shows the calculated effective dielectric constant (left hand vertical axis) and effective refractive index (right hand axis) as obtained numerically from band structures calculated at various r/a ratios. Values are given as a function of fill fraction for the two polarizations.

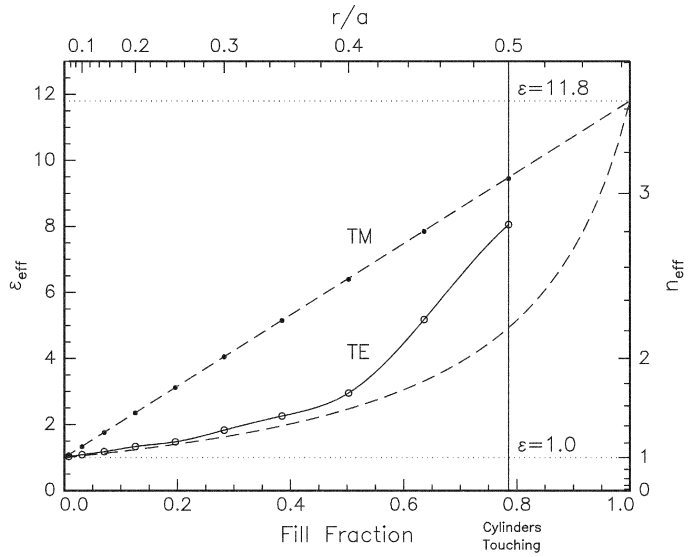

Fig. 5. Effective dielectric constant for a square lattice of silicon cylinders ($\varepsilon = 11.8$) in air ($\varepsilon = 1.0$). The effective dielectric constant was derived from separate band structure calculations at each fill fraction. The values obtained for TM polarization are shown by the solid dots, while the open circles show the results for TE polarization. The dashed line indicates the effective ε as calculated from Maxwell–Garnett effective medium theory. The solid line through the points for TE polarization is a guide to the eye.

Data are shown for TM (dots) and TE polarization (circles). The dashed lines correspond to the Maxwell–Garnett effective medium theory for the two polarizations. As can be seen, ε_{eff} for TM polarization increases linearly with fill fraction, in perfect agreement with effective medium theory although the theory is only exact for small fill fractions. The data for TE polarization show an initial slow increase with fill fraction, roughly equal to what effective medium theory predicts, followed by a much stronger increase for fill fractions above 0.5.

Similar calculations as in Fig. 5 were also performed for dielectric constants of the rods between 1.0 and 16.0. It was found that a linear increase in ε_{eff} was observed for TM polarization in all cases; the result for TE polarization was found to depend on both the fill fraction of rods and the dielectric contrast of the lattice. For r/a values above 0.5 a lattice of star shaped holes should be considered instead of dielectric cylinders.

To achieve (effective) index guiding in a 2D photonic crystal, it must be sandwiched between two layers of lower dielectric constant. In waveguide theory, TE and TM modes are defined as having their electric field (TE) or magnetic field (TM) transverse to the interfaces of the sandwich. Following this definition of waveguide modes for planar waveguide structures, the TE waveguide mode corresponds to the TE modes of the photonic crystal. For TM waveguide modes the electric field is nearly parallel to the long axis of the

cylinders. However, there is a small component (<10%) that is perpendicular to the cylinders. This can be seen directly when using the ray optic approach for waveguide modes in which the light is confined by total internal reflection of the rays. To calculate the effective index for TM waveguides we have neglected this small effect.

While the in-plane propagation of electromagnetic waves is predominantly described by the photonic band structure, the index guiding in the vertical direction is governed by the polarizability of the cylinders (Van de Hulst 1957). The average polarizability is given by the effective index calculated in the long wavelength limit. We can get an estimate of the vertical index guiding using the effective index calculated from the band structure as long as a significant amount of the electric field is contained in the dielectric cylinders, making our approach most valid for the first dielectric band. Although many practical devices make use of the PBG itself, where no propagating modes exist, our results can be used to estimate mode mismatch and coupling losses for devices with only a few rows of rods, or devices making use of the strong dispersion near the band-edge where propagating modes do exist. Our model gives a simple estimate of the required minimum length of the cylinders to prevent the light from leaking to the substrate in such a case. For devices employing higher lying bands our approach overestimates the index guiding, since a large fraction of the electric field is concentrated outside the dielectric cylinders.

In the following we will discuss three materials systems based on silicon in which index guiding in a 2D photonic crystal may be achieved. The first two rely on creating a spatial variation of the index along the Si pillars using either a-Si or SiGe. The third makes use of a SOI substrate where the Si pillars are placed on a planar insulator (SiO_2) layer, which has a significantly lower refractive index. For all these materials waveguiding in a channel waveguide was shown experimentally (Emmons *et al.* 1992; Cocorullo *et al.* 1998; Schüppert and Petermann 1998).

3.1. AMORPHOUS SILICON

Amorphous silicon (a-Si) can be made by ion irradiation of a single crystal Si (c-Si) substrate. We have studied 4 MeV Xe irradiation at 77 K that creates a 2 μm thick a-Si on c-Si. Structural relaxation at 500 °C for 2 h in a vacuum furnace was performed to remove point defects and to relax the a-Si network structure (Roorda *et al.* 1991). The refractive index of the a-Si layer was measured by variable angle spectroscopic ellipsometry (not shown) and is 3.73 at 1.5 μm, significantly higher than that of c-Si ($n = 3.45$). This result is similar to that found for a-Si made by ion irradiation using other ions (Waddell *et al.* 1984). Ellipsometry and transmission measurements on 2 μm

thick amorphous layers gave no indication for measurable optical absorption, from which we estimate that the absorption coefficient of amorphous silicon at 1.5 μm is smaller than $\sim$50 cm^{-1}. Hence, a-Si would be a suitable waveguide material in a photonic crystal with dimensions in the order of 10 μm. However the optical loss may still be significant for a cm long input/output waveguide integrated with the photonic crystal.

Using an a-Si top section of the pillars in a photonic crystal, the a-Si thickness and the pillar length (etch depth) should be chosen such that there is a minimal coupling to the bulk Si substrate. Considering only TM modes, the effective index of crystalline silicon cylinders at the optimum r/a of 0.18 is 1.45, as obtained from Fig. 5. Similarly the effective index for a-Si pillars with $r/a = 0.18$ is found 1.52.

Calculations to estimate the optical mode profile in the vertical dimension are shown in Figs. 6 and 7. Fig. 6a shows the solution of the propagation constant β, i.e. the component of the wavevector in the direction of propagation, for TM modes as function of the a-Si guiding layer thickness. The waveguide structure consists of crystalline silicon pillars ($n_{\text{eff}} = 1.45$) with an a-Si section ($n_{\text{eff}} = 1.52$), in air ($n = 1.00$). For an a-Si layer thickness up to 2.5 μm the planar waveguide structure only supports a single TM mode. The corresponding propagation constants in a planar waveguide made of a-Si on top of crystalline silicon are shown in Fig. 6b. Because of the large indices and relatively large index contrast, such a planar waveguide supports many modes and has propagation constants that differ very much from that of the PBG waveguide.

The field distribution of the zeroth order modes in the PBG waveguide are shown in Fig. 7. Modes are compared for three different a-Si thicknesses of 1.0, 2.0 and 2.5 μm. The modes were normalized such that the power flow for all the modes is the same. It can be seen from the figure that for a 1.0 μm thick a-Si layer the mode penetrates deep into the substrate. Thicker a-Si layers show better confinement for the zeroth order mode, such that almost all energy is confined within a layer of 5 μm long cylinders.

For practical applications one should keep in mind that deep anisotropic etching for the PBG structures is limited to an etch depth of $\sim$5 μm (Zijlstra *et al*. 1999). Amorphization up to a depth of 2 μm can be done using e.g. 4 MeV Xe ion irradiation into a planar Si wafer. Subsequently pillars can be etched, resulting in crystalline Si pillars with an a-Si top section. Therefore it is concluded that the fabrication of a structure based on a-Si should be possible.

As discussed earlier the propagation constant of the planar a-Si waveguide differs from that of the PBG waveguide. Because practical devices will most likely combine both planar waveguides and PBG waveguides it is important to consider the power coupling efficiency η between the planar waveguide and the PBG waveguide. We have assumed a butt-end coupling of the two waveguides. In that case the coupling efficiency η is given by (Pollock 1995):

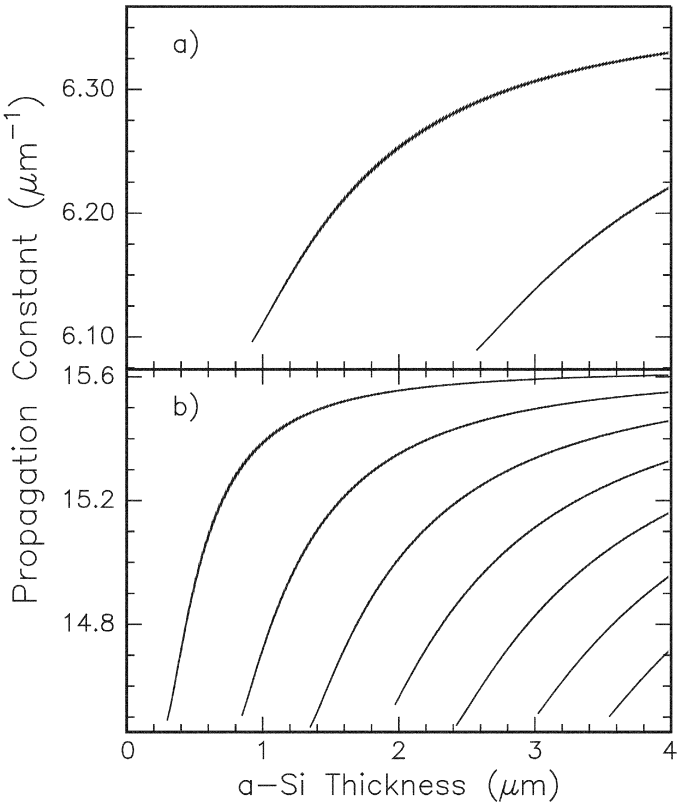

Fig. 6. Calculated propagation constant and waveguide modes for an a-Si/c-Si photonic crystal waveguide structure. (a) Propagation constant for the PBG structure, using effective indices of 1.52 and 1.45, as function of a-Si thickness. (b) Propagation constant for a planar waveguide of a-Si on c-Si as function of a-Si thickness.

$$\eta = \left| \frac{2\beta_i \beta_t}{(\beta_i + \beta_t)} \frac{1}{2\omega\mu_0} \int_{-\infty}^{\infty} E_i(x) E_t^*(x)\, dx \right|^2$$

where β_i and β_t are the propagation constants of the incoming and transmitted waveguide mode. E_i and E_t are the normalized electrical field amplitudes of the modes.

Using the calculated propagation constants for both the PBG waveguide and the planar waveguide the coupling efficiency between the fundamental modes was calculated for a 1.0 μm and a 2.0 μm thick a-Si waveguide. The calculated coupling losses expressed in dB are summarized in Table 1. As can be seen the coupling losses are larger for the 1.0 μm thick guide. This can be explained from the fact that in the PBG waveguide a large fraction of the mode propagates outside the guiding layer (mode confinement = 0.45, see

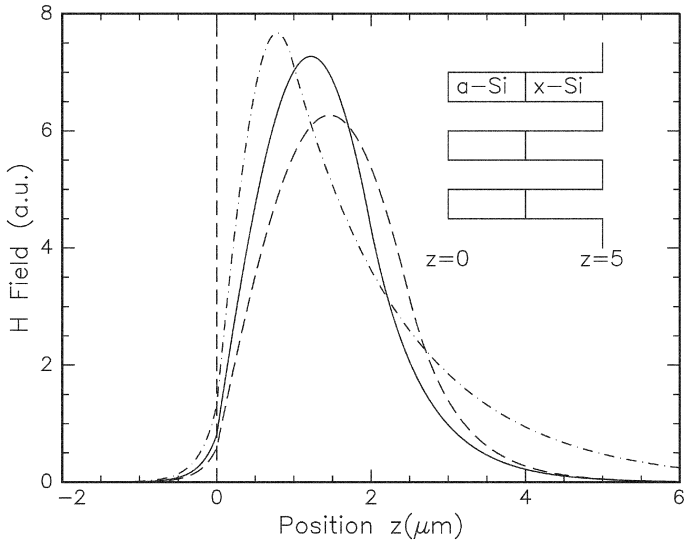

Fig. 7. Field strength of the calculated waveguide modes for a-Si thicknesses of 1.0 μm (—·—·), 2.0 μm (—) and 2.5 μm (- - -). The modes were normalized such that the power flow is the same for each mode.

Table 1. Comparison of the calculated coupling efficiencies η in dB for a-Si, SiGe and SOI waveguide structures

Waveguide material	r/a	Layer thickness d (μm)	Coupling efficiency η (dB)	Mode confinement Γ
a-Si	0.18	1.0	−3.6	0.45
	0.18	2.0	−1.3	0.90
$Si_{0.75}Ge_{0.25}$	0.18	2.0	−3.0	0.54
	0.18	4.0	−1.3	0.89
SOI	0.20	2.0	−1.1	0.90
	0.20	1.5	−1.9	0.70

The table shows the coupling efficiency and mode confinement for various thickness of the guiding layer thickness. The modes with good confinement have smaller coupling losses. The remaining coupling loss is mostly due to reflection.

Table 1) where the planar waveguide shows good confinement. The coupling losses for the 2.0 μm thick waveguide of −1.3 dB is partly due to a reflection of −0.9 dB caused by the difference in refractive index between the guiding layer of the incoming planar waveguide and the photonic crystal waveguide (we have only considered coupling losses between the fundamental modes, because coupling from a higher order mode to the fundamental mode leads to much higher coupling losses meaning that these modes do not propagate through the structure).

The rest of this paper summarizes the possibilities and coupling losses for similar structures, made using either SiGe on Si or SOI as a waveguide material. These results are summarized in Table 1 as well.

3.2. SILICON GERMANIUM

Silicon–germanium dielectric waveguides have been fabricated and show excellent transparency at 1.5 μm (Emmons *et al.* 1992), making SiGe an interesting candidate for photonic crystal waveguides. Here we consider the case similar as in Section 3.1 with pillars composed of a SiGe guiding top section on top of a Si pillar. The refractive index of the SiGe layer is higher than that of pure Si and depends on the atomic fraction of Ge. The band gap energy depends on the relative Si/Ge concentration and varies between the band gap of pure silicon (1.15 eV) and pure Ge (0.74 eV) for fully relaxed layers (Kasper 1995).

To fabricate structures with a similar index contrast as discussed for a-Si, a Ge atomic fraction of 50 at.% is needed. It is very difficult to fabricate SiGe waveguide layers with such a high Ge content on one hand and have low optical losses on the other hand (Emmons *et al.* 1992). We have therefore limited the atomic fraction of Ge to 25%. For a Ge content of 25 at.%, the $Si_{0.75}Ge_{0.25}$ layer has a refractive index of 3.53 and a band gap of 1.06 eV, corresponding to a wavelength of 1.17 μm in vacuum and will hence be transparent at 1.5 μm. For a PBG structure with $r/a = 0.18$ the effective index of the SiGe layer is 1.47, giving a relatively small index contrast with the pure Si pillars underneath ($n_{\text{eff}} = 1.45$).

Consequently the mode size for a 2.0 μm thick $Si_{0.75}Ge_{0.25}$ waveguide is bigger than that of a 2.0 μm thick amorphous waveguide and the mode is less well confined in the photonic crystal waveguide. Therefore a 2 μm thick SiGe waveguide leads to a relatively high coupling loss of −3.0 dB. The reflection loss of −0.8 dB is comparable to that of the a-Si waveguides. To improve the coupling the SiGe layer thickness can be increased to 4.0 μm giving a comparable coupling loss as the 2.0 μm thick a-Si waveguide as shown in Table 1. However, to avoid coupling to the substrate a total etch depth of 8–10 μm is required, making the fabrication of these SiGe structures less attractive.

3.3. SILICON-ON-INSULATOR

SOI is a commercially available material with high optical quality, consisting of a single crystal Si layer separated from the Si substrate by a SiO_2 layer. Devices can be made by etching cylinders in the thin Si layer only, leaving the SiO_2 layer intact. As already pointed out, the effective refractive index of a square array of crystalline Si cylinders is 1.45 for $r/a = 0.18$. The refractive index of SiO_2 is 1.45, which means that no index guiding can be achieved in an array of silicon pillars on SiO_2 with r/a smaller than 0.18. To achieve similar modes as calculated for a-Si one has to increase r/a such that the effective index increases to 1.52, corresponding to $r/a = 0.20$.

Commercially available SOI wafers using the 'smartcut' process typically have a maximum oxide thickness of 3 μm. The Si layer on top is limited to 1.5 μm, although it can be grown thicker using epitaxial growth. For our calculations we used a thickness of 2.0 μm as a starting point to compare the waveguiding properties with that of the a-Si structures. The results of the calculation are shown in Table 1. A 2.0 μm thick SOI layer with $r/a = 0.20$ has the same waveguide modes as an a-Si structure with $r/a = 0.18$. Therefore the mode overlap is the same. The difference in coupling efficiency with the a-Si structure is entirely due to a somewhat smaller reflection coefficient of −0.7 dB. For a layer thickness of 1.5 μm the mode confinement is smaller resulting in larger coupling losses.

For SOI structures the coupling losses can be further reduced by increasing the fill fraction of silicon. In this way the index contrast between the guiding layer and surroundings is increased leading to better confined modes with better overlap. In addition, the reflection loss is also reduced, because the refractive index difference between the incoming planar waveguide and the photonic crystal waveguide is reduced. For example for a 1.5 μm thick SOI layer with $r/a = 0.25$, the coupling loss is reduced to −0.6 dB, while the reflection is −0.5 dB. It should be noted however, that in this case both incoming and photonic crystal waveguides are multimode so that coupling between higher order modes should be considered. By definition these modes are less well confined (having a smaller propagation constant) and thus higher losses. In all the structures discussed we only considered propagation of TM polarized modes, because all layer thicknesses are still below the cut-off condition for TE modes in the photonic crystal waveguide.

4. Conclusions

Using the transfer matrix method we have explored the existence of PBGs for a square lattice of dielectric rods. Band gaps were only observed for TM polarization. By calculating the band structure as function of both the pillar r/a and the dielectric constant of the cylinders it was found that a minimum refractive index of 1.95 ($\varepsilon = 3.8$) is needed for a band gap at the optimum $r/a = 0.25$. For a higher dielectric constant of 11.8, corresponding to the dielectric constant of Si at 1.5 μm, the largest band gap was observed for $r/a = 0.20$, with a relative gap-width of 38%. Band structure calculations as function of r/a revealed up to four PBGs for TM polarization in a square lattice of silicon rods.

To design photonic crystal waveguides, the effective index was derived from the band structure calculations. For TM polarization the effective index corresponds to the result obtained from Maxwell–Garnett theory. We have calculated and compared waveguiding properties of photonic crystal wave-

guides operating around 1.5 μm using waveguide theory. Index guiding was achieved using a-Si, $Si_{0.75}Ge_{0.25}$ or SOI. It was concluded that the fabrication of a-Si and SOI structures is possible, while fabrication of SiGe structures is difficult because of the large etch depths needed. The coupling losses for butt-end coupling of a planar waveguide to a photonic crystal waveguide were found to vary between −1.1 and −3.6 dB, which can be explained from the difference in mode confinement of the photonic crystal waveguide. A large fraction of the coupling loss is caused by reflection losses which were found to vary between −0.9 dB for a-Si structures and −0.7 dB for SOI structures. Full 3D mode calculations are required to study the coupling in more detail.

Acknowledgements

Christof Ströhhofer and Pieter Kik are gratefully acknowledged for stimulating discussions on waveguide theory. This work is part of the scientific program of the foundation of fundamental research on matter (FOM) and was made possible by financial support of the Dutch organization for scientific research (NWO).

References

Astratov, V.N., D.M. Whittaker, I.S. Culshaw, R.M. Stevenson, M.S. Skolnick, T.F. Krauss and R.M. De La Rue. *Phys. Rev. B* **60** 16225, 1999.

Baba, T., N. Fukaya and J. Yonekura. *Elec. Lett.* **35** 654, 1999.

Bartha, J.W., J. Greschner, M. Puech and P. Maquin. *Microelectron. Eng.* **27** 453, 1995.

Charlton, M.D.B., S.W. Roberts and G.J. Parker. *Mat. Sci. Eng. B* **49** 155, 1997.

Charlton, M.D.B. and G.J. Parker. *MRS. Symp. Proc.* **486** 87, 1998.

Cocorullo, G., F.G.D. Corte, R. de Rosa, I. Rendina, A. Rubino and E. Terzini. *MRS Symp. Proc.* **486** 113, 1998.

Emmons, R.M., B.N. Kurdi and D.G. Hall. *IEEE J. Quant. Elec.* **28** 157, 1992.

Joannopoulos, J.D., R. D. Meade and J.N. Winn. *Photonic Crystals: Molding the Flow of Light*, Princeton University Press, Princeton, NJ, 1995.

Johnson, S.G., S. Fan, P.R. Villeneuve and J.D. Joannopoulos. *Phys. Rev. B* **60** 5751, 2000.

Kasper, E. *Properties of Strained and Relaxed Silicon Germanium*, INSPEC, London, UK, 1995.

Lin, S.-Y., E. Chow, V. Hietala, P.R. Villeneuve and J. D. Joannopoulos. *Science* **282** 274, 1998.

Megens, M., J.E.G.J. Wijnhoven, A. Lagendijk and W.L. Vos. *Phys. Rev. A* **59** 4727, 1999.

Mekis, A., J.C. Chen, I. Kurland, S. Fan, P.R. Villeneuve and J.D. Joannopoulos. *Phys. Rev. Lett.* **77** 3787 1996.

Pendry, J.B. and A. MacKinnon. *Phys. Rev. Lett.* **69** 2772, 1992.

Pollock, C.R. *Fundamentals of Optoelectronics*, Irwin, Chicago, USA, 1995.

Roorda, S., W. Sinke, J. Poate, D. Jacobson, S. Dierker, B. Dennis, D. Eaglesham, F. Spaepen and P. Fuoss, *Phys. Rev. B* **44** 3702, 1991.

Schüppert, B. and K. Petermann. *MRS Symp. Proc.* **486** 33, 1998.

Sprik, R., B.A. van Tiggelen and A. Lagendijk. *Europhys. Lett.* **35** 265, 1996.

Stoffer, R., H.J.W.M. Hoekstra, R.M. de Ridder, E. van Groesen and F.P.H. van Beckum. *Opt. Quant. Elec.* **32** 947, 2000.

Tachi, S., K. Tsujimoto, S. Arai and T. Kure. *J. Vac. Sci. Technol. A* **9** 796, 1991.
Tokushima, M., H. Kosaka, A. Tomita and H. Yamada. *Appl. Phys. Lett.* **76** 952, 2000.
Van de Hulst, H.C. *Light Scattering by Small Particles*, John Wiley & Sons, New York, 1957.
Waddell, C.N., W.G. Spitzer, J.E. Fredrickson, G.K. Hubler and T.A. Kennedy. *J. Appl. Phys.* **55** 4361, 1984.
Winn, J.N., R.D. Meade and J.D. Joannopoulos. *J. Mod. Opt.* **41** 257 1994.
Zijlstra, T., E. van der Drift, M.J.A. de Dood, E. Snoeks and A. Polman. *J. Vac. Sci. Technol. B* **17** 2734, 1999.